EAR CANAL DEFORMATIONS BY VARIOUS EARPLUGS: AN IN SITU INVESTIGATION USING MRI

Simon Benacchio[*1,2,3], **Arthur Varoquaux**[†4,5], **Éric Wagnac**[‡1,3], **Olivier Doutres**[§1], **Virginie Callot**[¶4,5], **David Bendahan**[‖4,5], **and Franck Sgard**[**2]

[1]École de technologie supérieure, 1100 Rue Notre-Dame O, Montréal, QC H3C 1K3

[2]Institut de recherche Robert-Sauvé en santé et sécurité du travail, 505 Boulevard de Maisonneuve O, Montréal, QC H3A 3C2

[3]Centre de recherche de l'Hôpital du Sacré Cœur de Montréal, 5400, Boulevard Gouin O, Montréal, QC H4J 1C5

[4]Aix Marseille Université, CNRS, CRMBM UMR 7339, Marseille, France

[5]APHM, Hôpital de la Timone, Pôle d'imagerie médicale, CEMEREM, Marseille, France

1 Introduction

To be efficient, a Hearing Protection Device (HPD) should be worn during the time the workers are exposed to high level noises. However, considering the corresponding hearing difficulties and/or physical discomfort, workers do not use HPDs properly and consistently. In the past, some indicators of physical (static pressure on the ear canal (EC) walls) [1] and auditory (insertion loss, occlusion effect) [2, 3] discomfort induced by earplugs (EPs) have been assessed using numerical models. However, the *in situ* deformation of EPs and tissues surrounding the EC has never been observed experimentally. These deformations could provide useful information to investigate how EPs and tissues should be modelled and characterized mechanically in order to predict EP efficiency indicators such as sound attenuation, occlusion effect and mechanical pressure applied on the EC walls. In this study, we assessed the deformation of the open and occluded EC of a single human subject using high-resolution magnetic resonance imaging (MRI) and for seven different EPs.

2 Method

2.1 Earplug insertion in the ear canal

Ear canal. The deformation of open and occluded EC was investigated for both ears. In order to raise the EPs conspicuity and the external auditory canal delineation, ECs were filled with natural almond oil.

Earplugs. Three groups of EPs were investigated: the moldable EPs made from polyvinyl chloride or polyurethane foam materials, the pre-molded EPs made from silicone or foam and plastic and the custom molded EPs made from silicone, acrylic or thermosoft materials. The seven EPs and a qualitative description of their rigidity and initial shape are presented in Table 1. A view of each EP is given in Figure 1.

Table 1: Description of the earplugs. The mathematical symbols (-/+) qualitatively sort the rigidity and initial shape of earplugs.

EP name (and type)	Materials (and rigidity)	EP/EC similarity
$\mathbf{M_f}$ (moldable)	foam (- -)	- -
$\mathbf{PM_s}$ (pre-molded)	silicone (-)	- -
$\mathbf{PM_{fp}}$ (pre-molded)	foam + plastic (-)	- -
$\mathbf{M_{s25}}$ (molded)	silic. shore A 25 (+)	++
$\mathbf{M_{s40}}$ (molded)	silic. shore A 40 (++)	++
$\mathbf{M_t}$ (molded)	thermosoft (+++)	++
$\mathbf{M_a}$ (molded)	acrylic (++++)	++

2.2 High-resolution magnetic resonance imaging

As few pathologies involve the outer ear, this part of the body has never been worthy of interest in MRI studies. Thus, a 3D space MRI sequence described in Table 2 has been optimized to non-invasively discriminate the tissues surrounding the EC. Using these parameters, the fat tissues and the almond oil appear white on images, the skin and the cartilaginous parts appear grey and the bones, the foam, the plastic, the acrylic, the thermosoft material and the air appear black (see for example Fig. 1(b)). Given the relatively small diameter of the RF coil (20 cm) as compared to the cranial diameter, the left and right pinna of the subject were slightly deformed during MR acquisitions. Moreover, ear muffs were used during open EC measurements to protect the subject from the MR system noise. In this case, the pinnae of the subject were largely deformed. However, according to first observations, it was considered that, from the concha to the eardrum, the EC deformation due to the RF coil and ear muffs was small enough and thus acceptable.

Table 2: Main parameters of the optimized MRI sequence.

MR system	Siemens 3T (Verio)
Radiofrequency (RF) coil	Head 32 channels
Sequence	Space 3D
Weighting	T1
Plane	Axial
Slices	128
Resolution [mm]	0.6 iso.
Acquisition time [min]	9

2.3 MRI post-processing

To accurately estimate the EC deformation, all images have been repositioned using a rigid registration method from the *Advanced Normalization Tools (ANTs)* library toolkit [4]. Then, each EC was segmented using one slice of the axial plane. This slice was arbitrarily chosen to observe the EC deformation for each EP and is presented in Figure 1. The boundaries of the segmentation were given by the EC walls and a sagittal plane located in the concha. On the one hand,

[*]Simon.Benacchio@irsst.qc.ca

[†]DamienArthur.VAROQUAUX@ap-hm.fr

[‡]Eric.Wagnac@etsmtl.ca

[§]Olivier.Doutres@etsmtl.ca

[¶]Virginie.CALLOT@univ-amu.fr

[‖]david.bendahan@univ-amu.fr

[**]Franck.Sgard@irsst.qc.ca

this plane was chosen to observe the largest part of the EC and, on the other hand, to avoid the deformation due to the RF coil and ear muffs. The example of the open EC segmentation is given by the red area in Figure 1(b). Finally, the EC deformation was related to the number of voxels of each segmentation and qualitatively evaluated by a radiologist.

3 Results and discussion

Figures 1(a) and 1(b) show the non occluded (**NO**) EC. The other images present the rigidly registrated occluded EC using the moldable (Fig. 1(c) and 1(d)), pre-molded (Fig. 1(e) and 1(f)) and custom molded (Fig. 1(g), 1(h), 1(i) and 1(j)) EPs. The images are displayed using *FSLView* [5]. Table 3 gives the segmented number of voxels for both open and occluded ECs. The deformation of the EC clearly depends on the type of EP. According to the number of voxels given in Table 3, the moldable EPs and the $\mathbf{PM}_{fp}$ pre-molded EP apply the largest deformation on the EC. Then, the deformation decreases using the $\mathbf{PM}_{s}$ pre-molded, and the molded EPs respectively. Using the pre-molded EPs, the EC fits the shape of the round and conic EPs as shown in Figure 1(e) and 1(f) respectively. The custom molded EPs induce the smallest but non negligible deformation of the EC as they are made to fit its shape. Note that these observations are only valid for the slice of interest.

Table 3: Number of voxels for the segmentations of the open and occluded ECs.

EP (right)	**NO**	$\mathbf{M}_{f}$	$\mathbf{PM}_{fp}$	$\mathbf{M}_{s25}$	$\mathbf{M}_{a}$
Voxels	141	332	330	281	290
EP (left)	**NO**	$\mathbf{M}_{f}$	$\mathbf{PM}_{s}$	$\mathbf{M}_{s40}$	$\mathbf{M}_{t}$
Voxels	196	302	280	254	232

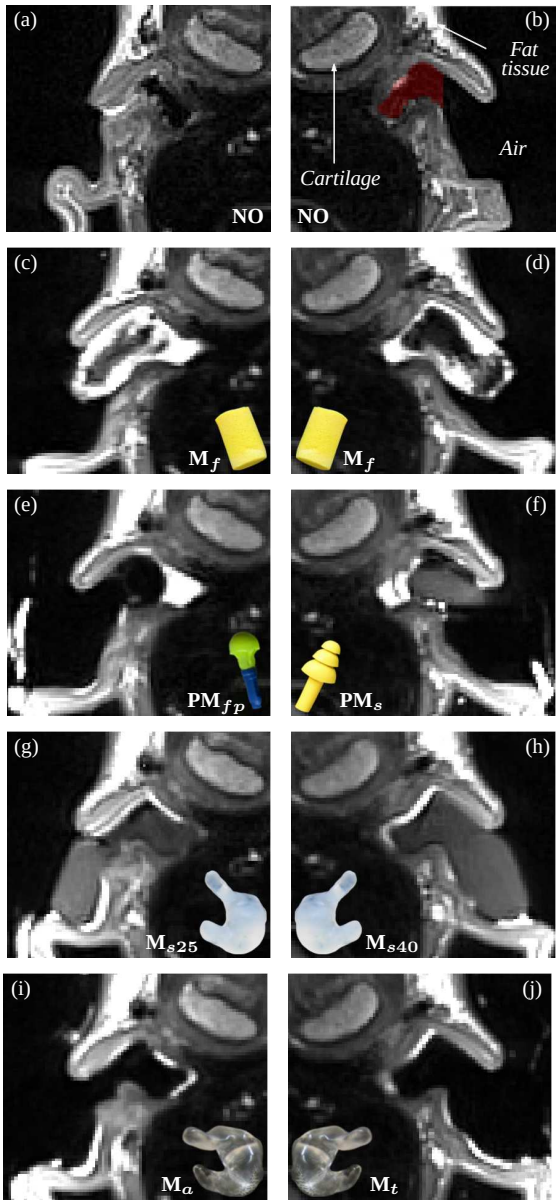

Figure 1: Reference images: (a,b) right and left non occluded (**NO**) ear canal (EC). Rigid registration of the EC occluded by different earplugs: (c,d) moldable ($\mathbf{M}_{f}$), (e,f) pre-molded ($\mathbf{PM}_{fp}$ and $\mathbf{PM}_{s}$), (g,h) molded silicone ($\mathbf{M}_{s25}$ and $\mathbf{M}_{s40}$), (i,j) molded acrylic and thermosoft ($\mathbf{M}_{a}$ and $\mathbf{M}_{t}$). $\mathbf{PM}_{fp}$, $\mathbf{M}_{a}$ and $\mathbf{M}_{t}$ are non visible on MR images but a view of each earplug is given in the bottom corner of images. The red area in Figure (b) shows the segmentation of the open EC.

4 Conclusions

This pilot study aimed at observing the deformations of the ear canal by seven different earplugs. Magnetic resonance images providing a good contrast between the tissues surrounding the ear canal were acquired to non-invasively characterize these deformations. Using segmentations of the open and occluded ear canal within one slice of the axial plane, we identified the largest deformations with the moldable and the round pre-molded earplugs, while they were smaller with the other pre-molded and the molded earplugs. However, it is not possible to conclude on the global deformation of the EC since only one slice is used for segmentation. The next step of the study is to compute a quantitative analysis on the global deformation of both EPs and EC using non linear registration methods.

Acknowledgments

This work was founded by the Institut de recherche Robert-Sauvé en santé et sécurité du travail. The authors would like to thank Arnaud Le Troter for his help with post-processing.

References

[1] A. T. Baker, S. H. Lee, and F. Mayfield. Evaluating hearing protection comfort through computer modeling. *2010 SIMULIA Customer Conference*, 2010.

[2] G. Viallet, F. Sgard, F. Laville, and J. Boutin. A finite element model to predict the sound attenuation of earplugs in an acoustical test fixture. *J. Acoust. Soc. Am.*, 136(3):1269–1280, September 2014.

[3] M. K. Brummund, F. Sgard, Y. Petit, and F. Laville. Three-dimensionnal finite element modeling of the human external ear: Simulation of the bone conduction occlusion effect. *J. Acoust. Soc. Am.*, 135(3):1433–1444, March 2014.

[4] B. B. Avants, N. J. Tustison, G. Song, and J. C. Gee. Ants: Advanced open-source normalization tools for neuroanatomy. *Penn Image Computing and Science Laboratory*, 2009.

[5] M. Jenkinson, C. F. Beckmann, T. E. Behrens, M. W. Woolrich, and S.M. Smith. Fsl. *Neuroimage*, 62(2):782–790, 2012.